The suitability of High Temperature – Aquifer Thermal Energy Storage in Holland-Rijnland

By:
Rein de Voogd
4374452

Supervisors:
Dr. Ir. Martin Bloemendal
Dr. P.J. Vardon

Civil engineering and Geosciences

June 2019

Abstract

High Temperature – Aquifer Thermal Energy Storage (HT-ATES) is a way to efficiently store heat with use of the subsurface. Region Holland-Rijnland has the vision to be free of the use of natural gas in 2050. A proposed high temperature heating network from the port of Rotterdam to the households of Leiden, combined with the use of an HT-ATES system as a buffer, could be the next step to achieve the laid-out vision. This research is a first step in the possibility of placing an HT-ATES system near Leiden. An interpretation of the subsurface near Leiden is done based on information from DINOloket to find potential formations and aquifers. Then, combined with different scenarios for the heat demand from the proposed heat network, a preliminary design of an HT-ATES system is made to test the viability of the potential aquifers. The most suitable aquifer is found in the Maassluis formation at a depth of 230 meters. Per scenario, this aquifer needs the least number of wells for the desired pumping rate. Depending on the scenario, the aquifer has a thermal recovery efficiency ratio between 0,16 – 0,26 and an area – to – volume ratio between 0,051 – 0,056. Other suitable aquifers can be found in the Maassluis formation at a depth of 170 meters and in the Oosterhout formation at a depth of 320 meters. The subsurface near Leiden is suitable for an HT-ATES system, but more research needs to be done on the conflict between heat supply from the port of Rotterdam and heat demand from the proposed network in order for an HT-ATES system to fully supply the seasonal heat demands.

Acknowledgements

Firstly, I want to thank my supervisors Dr. Ir. Martin Bloemendal and Dr. Phil Vardon. Every week a meeting was held that helped me guide the project to its completion. During times when I was stuck, I even could visit Dr. Ir. Martin Bloemendal outside meeting hours to gain help in solving the situation. I appreciate the guidance and help very much. Secondly, I want to thank Martijn Romijn from Holland-Rijnland for giving me insight into the project considering the high temperature heat network from the Port of Rotterdam. Without this insight, this thesis would not be possible.

Finally, I want to thank my family and friends for setting my head straight at the end of a hard week of work.

Rein de Voogd

Contents

1: Introduction

1.1 Problem description

The demand for a more renewable and environmentally friendly energy source is increasing by the years [1]. This is due to our reliance upon fossil fuels such as oil and natural gas negatively affecting the planet. Burning these fossil fuels increases the amount of carbon dioxide (CO_2) that is released into the atmosphere, leading to a heightened greenhouse effect and warming of the earth [2].

In 2019, the main energy source in Europe is still fossil fuels [3]. This is also the case for the Netherlands [4]. Households in the Netherlands take up 28% of the total energy consumption [5]. Of this 28%, a total of 71% is used for heating the household [5]. From this 71%, a total of 87% is generated via the use of natural gas [5]. The goal for the Dutch government is to have a 95% reduction in CO_2 emission by 2050 [6]. Clearly, reducing natural gas usage will reduce CO_2 emission.

Like the rest of the Netherlands, also region Holland-Rijnland is to be made free of the use of natural gas. The vision of region Holland-Rijnland, is to be free of the use of natural gas in 2050 [7]. To get this accomplished, a more renewable and environmentally clean energy source needs to be put in place.

One of the alternatives is to connect more households to a high temperature heating network. A high temperature network delivers hot water of minimal 70 °C to households. In 2016, an agreement was made to secure this heat supply in the future and making it more sustainable through the construction of a heat pipeline from the Port of Rotterdam. This pipeline has to transport residual industrial heat from the Port of Rotterdam to, among other places, households in Leiden. But its capacity is bigger than is necessary for Leiden's need only and there is an excess capacity that could be used for other cities in Holland-Rijnland. This study is performed to help optimize the capacity of that pipeline by means of storing the excess heat that can be transported in summers for use in winters, in order to make the pipeline's heat available for as many households in Holland-Rijnland as possible.

The transition from individual gas boilers to the heating network requires considerable investments. Important is that the connections to the heat network should be a more financially attractive option than the existing gas one. To make this possible a whole package of measures is needed. One of these measures is the use of High Temperature – Aquifer Thermal Energy Storage (or HT-ATES for short). The problem that is surveyed in this study is that it is yet unknown if the underground under the projected pipeline is suitable for this kind of storage.

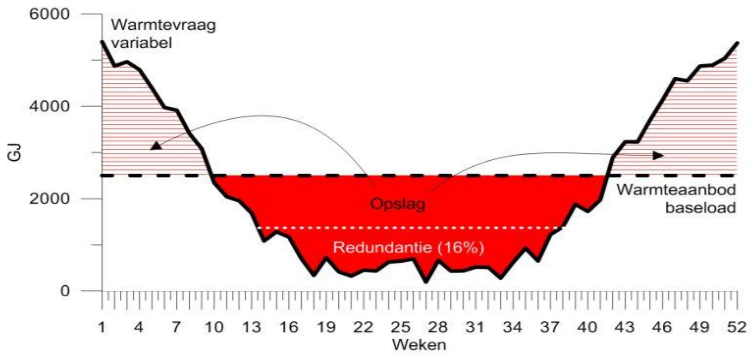

Figure 1: Graph showing variation in heat demand in between seasons (Hartog et al., 2016)

Throughout the year, heat supply is constant. Heat demand however, varies in between seasons, as illustrated by figure 1. HT-ATES makes it possible to store heat during low seasonal heat demand. This storage can then be used as a buffer for use during high seasonal heat demand. With this system, heat supply can be delivered more efficiently. A lower heat supply will reduce the costs, making the system a more financially attractive option.

1.2 Goal

The goal of this research is to see if the deep underground near Leiden is suitable in order to store the heat supplied from the port of Rotterdam. This report should serve as a starting point for further, more detailed research concerning HT-ATES in Holland-Rijnland.

1.3 Approach

First, background information is given in chapter two. In chapter three, possible heat storage will be computed. Heat demand throughout the year is computed to find out the time period for potential buffering. With these values known, possible storage is computed. In chapter four, the geology of the subsurface of the proposed area for the heat network is investigated. This is done by describing the ideal geologic setting for an aquifer needed for an HT-ATES system. Then, the subsurface of the area considered for the high temperature network will be interpreted to find possible formations and aquifers. Chapter five consists of a preliminary design of the HT-ATES system. The number of wells. and different ratios are computed to find out which potential aquifer is the most suitable for use of an HT-ATES system. Chapter six describes the challenges in designing an HT-ATES system. Chapter seven will discuss the report and recommendation are given for further research. Finally, a conclusion will be made for the suitability of an HT-ATES system near Leiden.

2: Background Information

Aquifer Thermal Energy Storage, or ATES for short, is already a common way to store energy in the Netherlands. This chapter provides an explanation on how an ATES system works. The definition of an HT-ATES, MT-ATES and a LT-ATES will be explained, and an explanation on which system needs to be used for this heat network. To understand the geologic terms used in this report, a small elaboration on the basic geology will be given.

2.1 ATES

Heat demand throughout the year varies per season. During summertime, heat demand is in its lowest. Due to higher outside temperatures, heating of the household is not required. Most of the heat demand consists only for cooking and heating of water used for showers, tap water, etc. During wintertime heat demand reaches its peak. The outside temperatures are now lower, and households need to be heated. ATES systems can store thermal energy during low heat demands in the summertime. This stored heat can then be used to supply the peak heat demand during winter time. ATES systems can store geothermal heat, solar heat, and in the case of region Holland-Rijnland, residual industry heat. Next to heat storage, HT-ATES can also store excess cold water during wintertime to be reused for cooling of buildings during summertime.

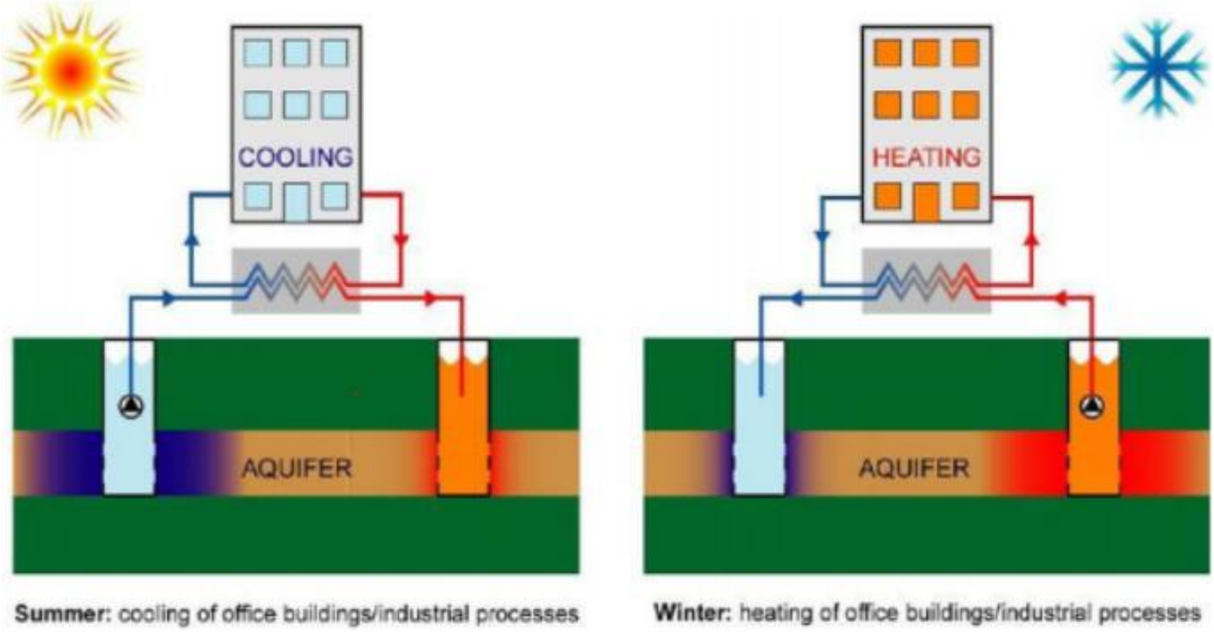

Figure 2: Illustration of how an HT-ATES System works (Salcedo Rahola et al.)

Figure 2 illustrates how an HT-ATES system works. During summertime, outside temperatures are higher and the building needs cooling. The cold well extracts cold water stored during the summer and cools the building. Through exchange of heat, the water heats up. The water is then injected via the warm well for later use during wintertime. During wintertime, outside temperatures are lower and the building now needs heating. The same process occurs, but done the other way around.

To store and recover the heat, ATES systems extract hot water and inject cold water in and from aquifers using geothermal wells. Therefore, operating an ATES system uses the subsurface as a temporal storage mechanism to buffer the low demand in summertime to provide peak demand in wintertime. This makes the heating network a more financially attractive option, due to the more efficient use of heat supply throughout the year. It also decreases the amount of CO_2 emitted in the atmosphere, due to the use of a more cleaner energy source.

2.2 HT- ATES and LT-ATES

In general, there are three types of ATES systems: Low Temperature – Aquifer Thermal Energy Storage (LT-ATES), Middle Temperature – Aquifer Thermal Energy Storage (MT-ATES) and High Temperature – Aquifer Thermal Energy Storage (HT-ATES). They are distinguished by the temperature of the water stored in the aquifer. In a LT-ATES, temperatures stored are lower or equal than 30°C. In a MT-ATES, temperatures stored are between 30-60 °C. In a HT-ATES, temperatures stored are higher or equal than 60°C. In the case of the heat network in Leiden, heat of 70-90°C will be supplied from the port of Rotterdam. Thus, in order to store heat during summertime, an HT-ATES system should be in place.

2.3 Basic geology

2.3.1 Permeability

Permeability is a measure of the ability of a porous material (in this case: an underground sedimentary layer) to let fluid flow through the material. Permeability is influenced by the shape of the grain, porosity of the layer and the heterogeneity of the particle size. The SI unit for permeability is m^2. Permeability often gets described in terms of hydraulic conductivity. Permeability is a property of the porous medium itself while hydraulic conductivity is the property of the whole system including both porous medium and the flowing fluid. Often hydraulic conductivity is described in Darcy (D) or meters per day (m/d).

2.3.2 Porosity

Porosity is described as the amount of void spaces in a material. In the case of this report, the material considered is a sedimentary layer underground. Mathematically it can be described as follows (2.1):

$$Porosity = \frac{V_{pores}}{V_{grains}} * 100\ \% \qquad (2.1)$$

From this mathematical equation, it can be noted that porosity is expressed in percentages. Porosity is influenced by the grain distribution. Materials that consist of big particles can have a big volume of voids, but if these voids are filled with smaller particles, the porosity will be influenced negatively.

2.3.3 Aquifers

An aquifer is an underground sedimentary layer consisting of sand, gravel or a permeable rock. In general, there are two types of aquifers: unconfined aquifers and confined aquifers. An unconfined aquifer is not confined by an impermeable layer, or a cap layer. A confined aquifer does have a cap layer with low permeability on top of the aquifer. In the case of an HT-ATES system, a confined aquifer is preferred. This is to prevent the hot water stored in the aquifer to flow to other layers.

3: Required storage volume

In this chapter, the required storage volume will be discussed. Different scenarios in heat demand throughout the year required from the heat network will be computed. Then, potential heat storage and pumping rates per scenario will be computed.

3.1 Heat demand throughout the year

3.1.1 Total Heat demand per year

Holland-Rijnland [8] already has done research on the potential heat demand per year required from the heating network from the port of Rotterdam. From this research, multiple scenarios were gained for the potential heat demand. Table 1 shows the heat demand for a year per different scenario. The scenarios differ in the number of households and companies connected to the heat network and the use of potential local heat sources.

Scenario 1, a Business as Usual scenario, shows heat demand when 50% of the housing corporations, 25% of the particular households and 15% of the companies in the region are connected to the heating network and there is no use of local heat sources.

Scenario 2, the expected scenario, shows heat demand when 80% of the housing corporations, 50% of the particular households and 50% of the companies in the region are connected to the heating network and there is no use of local heat sources.

Scenario 3, the same expected scenario, has the same amount of connections to heat network as scenario 2, but makes use of potential local heat sources to decrease heat demand. Local heat sources decrease the heat demand down to 70 MWth per year [8]. However, if local heat sources are used, an increase in water volume in the aquifer needs to be taken into account due to the extra buffering required of those local heat sources. Thus, for further calculations using this scenario, 50% of the decrease in heat demand is assumed to be used for extra buffering of the local heat sources, which comes down to a heat demand of 108 MWth per year for scenario 3.

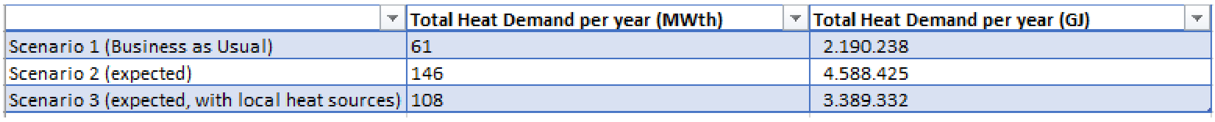

	Total Heat Demand per year (MWth)	Total Heat Demand per year (GJ)
Scenario 1 (Business as Usual)	61	2.190.238
Scenario 2 (expected)	146	4.588.425
Scenario 3 (expected, with local heat sources)	108	3.389.332

Table 1.: Total Heat demand per year for each different scenario in MWth and GJ respectively.

3.1.2 Heat demand per month

Heat demand varies throughout the year. As discussed before in chapter 2, heat demand peaks during wintertime and is at a low during summertime. In order to find out what the heat demands are per month, average outside temperatures per month need to be known. These averages are gained by averaging the outside temperatures per month from the weather station in Rotterdam [9] during the period from 2010 till 2018. An estimation is made that at an outside temperature of 12°C, heating of buildings will start. Then, a percentage from the total heat demand is computed that indicates the amount of heat needed to heat the building for that month using equation (3.1):

$$\text{Percentage heating building} = \frac{12 - T_{avg}}{\Sigma(12 - T_{avg})} * 100\%, \;\; T_{avg} < 12 \tag{3.1}$$

Where T_{avg} is equal to the average temperature per month in degrees Celsius (°C). The percentages per month are indicated in table 2.

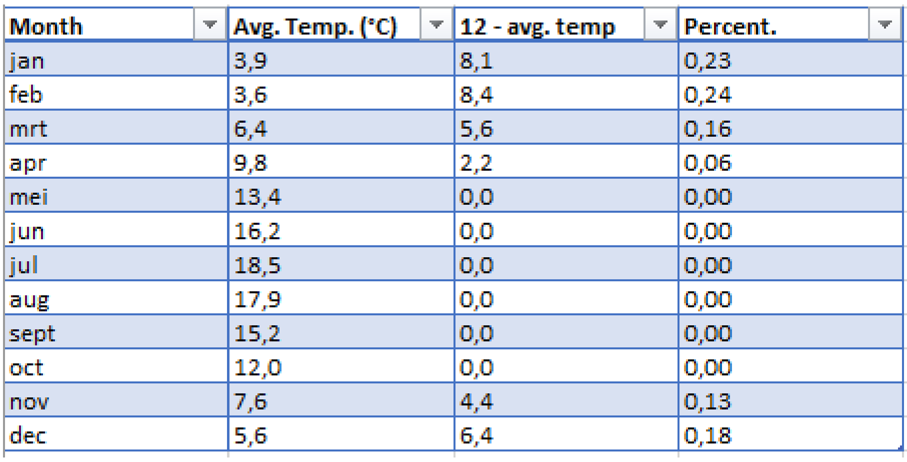

Month	Avg. Temp. (°C)	12 - avg. temp	Percent.
jan	3,9	8,1	0,23
feb	3,6	8,4	0,24
mrt	6,4	5,6	0,16
apr	9,8	2,2	0,06
mei	13,4	0,0	0,00
jun	16,2	0,0	0,00
jul	18,5	0,0	0,00
aug	17,9	0,0	0,00
sept	15,2	0,0	0,00
oct	12,0	0,0	0,00
nov	7,6	4,4	0,13
dec	5,6	6,4	0,18

Table 2: Average outside temperatures per month and the percentage of heat needed to warm up the building per month

Months that use 0% of the heat demand for heating of the building, heat demand only consists of heating of tap water, showers, etc. Heat demand for this usage is estimated to be 20% of the total heat demand per year. Heat demand per month for this usage is computed using equation (3.2):

$$Q_{non-heating} = \frac{(Q_{demand,year} * 0.2)}{12} \tag{3.2}$$

With $Q_{demand,year}$ being the total heat demand per year in joules (J) and $Q_{non-heating}$ being the heat demand for usage of heating of tap water, showers, etc. per month in joules (J)

From table 1, table 2 and equation (3.2) heat demand per month for the different scenarios can be computed and illustrated via graphs. These figures can be found in Appendix A.

3.2 Potential Storage and pumping rates

From previous research done by Holland- Rijnland [8], it is known that the yearly heat supply from the Port of Rotterdam consists of 62 MWth or 1955 TJ at maximum capacity. This comes down to a supply of 163 TJ per month. Total heat storage for an HT-ATES system for the different scenarios can now be computed by subtracting the heat demand per month from the heat supply per month and adding up the netto positive values.

From this heat storage, the equivalent volume of water needed to store the heat in the HT-ATES buffer can be computed using equation (3.3):

$$V = \frac{Q_{stored}}{c * \Delta T} \tag{3.3}$$

With V indicating the volume of water needed to store the heat in cubic meters (m^3), c the volumetric heat capacity of 4,18 MJ/(m^3*K) [10] and ΔT the temperature difference between the extraction- and injection well.

From previous research from Holland-Rijnland [8] it is known that hot water will be delivered with a temperate between 70-90 °C. From this, ΔT values of minimum 25 °C and maximum 35 °C can be assumed.

The pumping rates for the different scenarios can be computed using equation (3.4):

$$Q = \frac{P_{peak}}{c * \Delta T} \qquad (3.4)$$

Where Q is equal to the pumping rate in (m^3/s) and P_{peak} is peak power in Watts (W). P_{peak} can be computed using equation (3.5):

$$P_{peak} = \frac{Q_{stored}}{t} \qquad (3.5)$$

Where P_{peak} is peak power in Watts (W), Q_{stored} is the total heat storage in joules (J) and t representing the amount of time that ATES system is working at full capacity (s).

Tables 3 till 5 give an overview for the minimum and maximum amount of volumes of water that need to be stored and minimum and maximum pumping rates per different scenario. The values are computed using the previously mentioned equations. The volumes computed are only injected volumes, without consideration of losses and porosity.

N.B.: One might expect a higher peak power for scenario 2 and scenario 3 based on the total heat demand per year from table 1. However as can be seen from appendix A, the heat that can be stored for scenario 2 and 3 during summertime is lower than in scenario 1. Higher heat demands during summertime for scenario 2 and 3 causes lower possible storage of heat during summertime. In the calculation of the peak power, it is assumed that the heat stored during summertime is equally distributed per month that the ATES system works at full capacity, which are the months during wintertime. This leads to peak power being lower for scenario 2 and 3 compared to scenario 1.

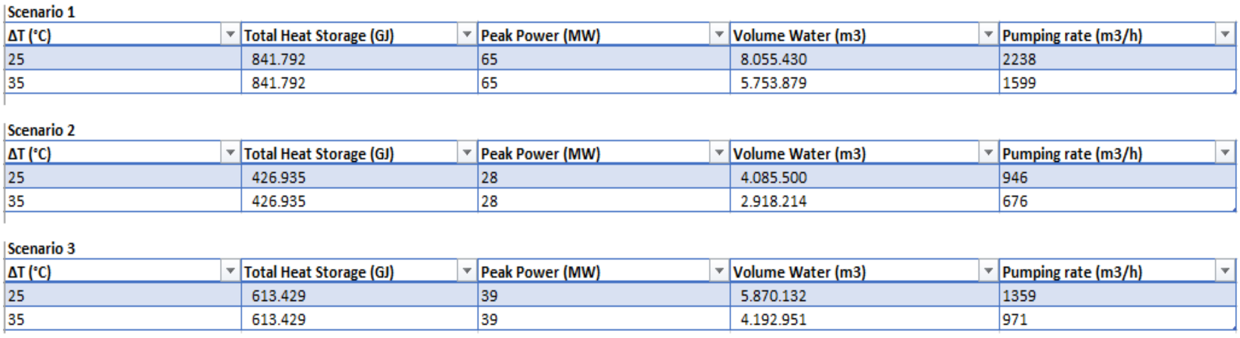

Scenario 1

ΔT (°C)	Total Heat Storage (GJ)	Peak Power (MW)	Volume Water (m3)	Pumping rate (m3/h)
25	841.792	65	8.055.430	2238
35	841.792	65	5.753.879	1599

Scenario 2

ΔT (°C)	Total Heat Storage (GJ)	Peak Power (MW)	Volume Water (m3)	Pumping rate (m3/h)
25	426.935	28	4.085.500	946
35	426.935	28	2.918.214	676

Scenario 3

ΔT (°C)	Total Heat Storage (GJ)	Peak Power (MW)	Volume Water (m3)	Pumping rate (m3/h)
25	613.429	39	5.870.132	1359
35	613.429	39	4.192.951	971

Tables 3 till 5: Volume of water that needs to be stored and the accompanying pumping rate per scenario

4: Geology

In this chapter, possible aquifer(s) for an HT-ATES system in the subsurface near Leiden will be located. This will first be done by describing the ideal geology for an aquifer. Then, an interpretation will be done of the subsurface near Leiden. Finally, the description of an ideal geology and the interpretation of the subsurface will be combined to find suitable formations and aquifers for an HT-ATES system.

4.1 Ideal geology of an aquifer for HT-ATES

In general, the ideal geology for an aquifer usable for an HT-ATES system should be as follows:

Porosity

Porosity indicates the amount of void spaces in the underground sedimentary layer. Thus, to have the highest storage capacity possible, the layer should have the highest porosity possible

Vertical conductivity

The vertical conductivity of the layer should be as low as possible, to decrease the occurrence of a thermal front during pumping of hot water in the aquifer [11].

Horizontal conductivity

In the case of high temperature storage, the horizontal conductivity of the layer should preferably be as high as possible. This is to increase the pumping capacity [11]. Realistic values will be between 3 - 15 m/d [12].

Cap layer

The cap layer should be positioned above the aquifer and should have a low permeability. This is to prevent the hot water stored in the aquifer to flow to other layers.

Heat Capacity

The layer should have a high heat capacity. The layer should not be able to change its base temperature rapidly due to the amount of hot water that get puts in to it. This is to prevent potential heat losses from occurring.

Depth

The depth of the layer should not be located below 500 meters. This is for a few reasons:

- Financially, this is due to the increase in cost of drilling at higher depths.
- Scientifically, a decrease of permeability and porosity occurs with depth.
- Legally, the legality becomes an issue due to the unclarity of the Mining law and Water law. Depending on the depth, it is prohibited without a license to detect terrestrial heat or explore geothermal heat [13].

The layer should also not be located shallower than 150 meters. This is to avoid heating of the subsurface [12].

Thickness

The aquifer should be thick enough to bear the amount of water needed to buffer seasonal demands with minimal heat losses and should at least have a thickness of 20 m [14].

4.2 Interpretation of the subsurface near Leiden

4.2.1 Identification of suitable aquifer in region Holland-Rijnland

Figures showing the area considered for the high temperature heat network and a proposed heat network throughout the area can be found in appendix B.1 till B.3. The ATES system should be easily accessible for the transport pipelines to distribute the stored heat to the households connected to the heating network. Appendix B.3 shows that the pipelines form a crossroads between Leiden, Leiderdorp and Oegstgeest. Geographically, positioning a buffer between these places would make for an ideal position to distribute the heat stored from the ATES to the households connected to the heating network. The geological viability is tested by taking cross sections in DINOloket [15].

4.2.2 Cross sections

To interpret the subsurface under the crossroads, cross sections are taken along the lines indicated in Appendix B.3. Cross sections are taken using DGM v2.2 and REGIS II v2.2.

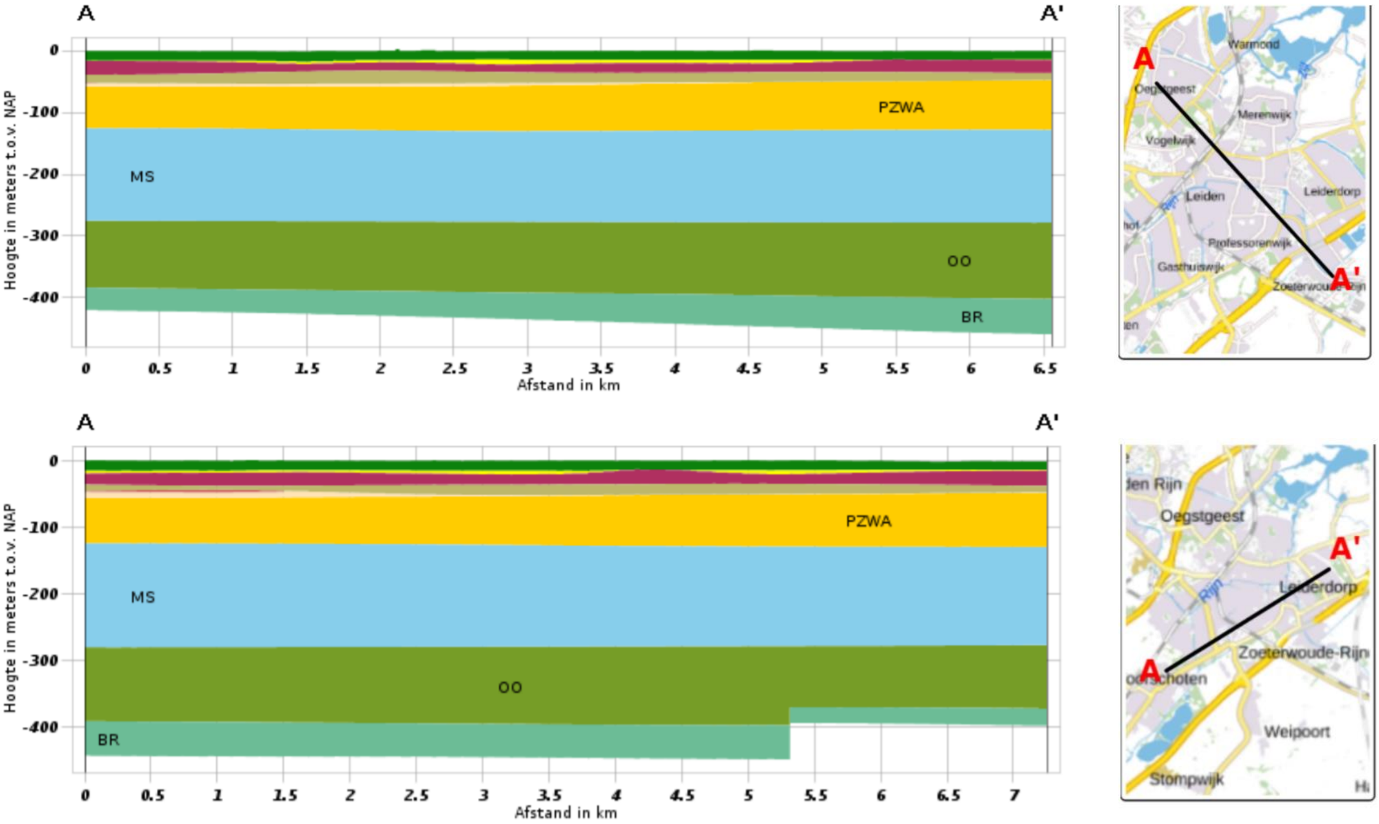

Figure 3: Cross sections taken through the proposed area obtained via DGM v2.2 in Dinoloket

Cross sections from figure 3 are obtained via DGM v2.2. The cross sections give information up until around 460 meters. Figure 3 shows two formations that need to have a closer look: the Maassluis formation and the Oosterhout formation.

4.2.3 Maassluis formation

This formation is situated below the formation of Peize and starts around a depth of 130 meters and has a thickness of 150 meters. According to DINOloket [16], this formation is described as a marine deposition dominated by calcareous, extremely fine to coarse sands. It also consists of silty, calcareous clay.

4.2.4 Oosterhout formation

This formation is situated below the Maassluis formation and starts around a depth of 280 meters and has a thickness of 115 meters. According to DINOloket [17], this formation is described as a marine deposition dominated by extremely fine to extremely coarse sands. It also consists of weak to strongly silty clay.

4.3 Suitable formations

4.3.1 Closer look at the formations using REGIS II v2.2

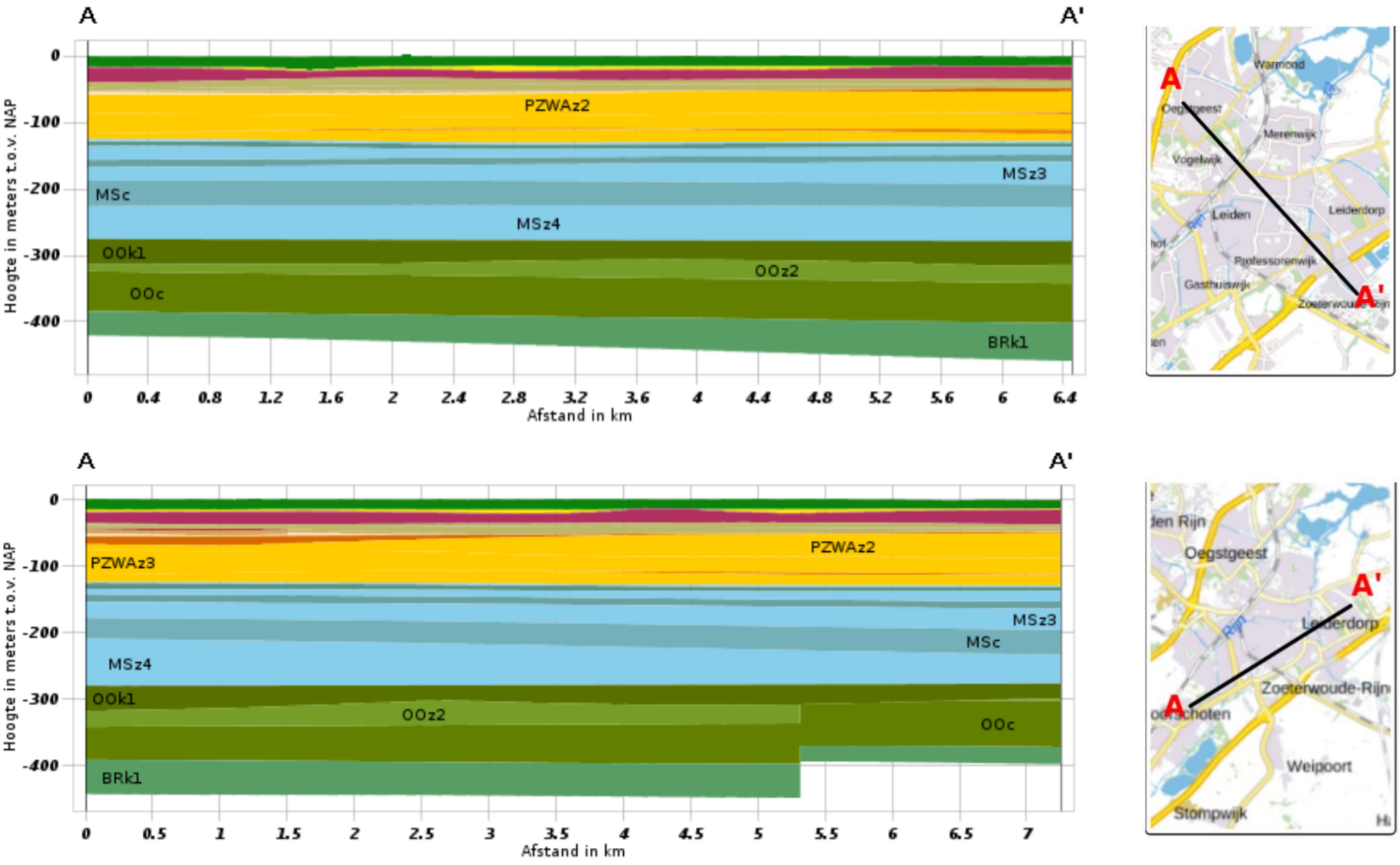

Figure 4: Cross sections taken through the proposed area obtained via REGIS II v2.2 in Dinoloket

Cross sections from figure 4 are obtained via REGIS II v2.2 and can be read via the legend found in appendix B.4. This model gives information up until around 460 meters, but goes more into detail into the formations. It shows which part of the formation is sandy, which part consists of clays or a combination of both. Figure 4 shows three possible aquifers: two possible aquifers in the Maassluis formation and one possible aquifer in the Oosterhout formation.

The first possible aquifer is located in the Maassluis formation. The aquifer starts at around 170 meters and has a thickness between 20 – 35 meters. The Aquifer predominately consists of sand with a small cap layer of predominantly clay above with a thickness between 8 – 10 meters. The thickness of this aquifer varies by quite a lot, being thinner near Oegstgeest and becoming thicker near Leiden, reaching its thickest point near Zoeterwoude.

The second possible aquifer is also located in the Maassluis formation. The aquifer starts at around 230 meters and has a thickness between 40 – 50 meters. The Aquifer predominately consists of sand with a complex cap layer of sand and clay above with a thickness between 25 – 30 meters. The aquifer becomes less thick when it reaches Leiderdorp, but still remains thick enough to match the standards of an ideal geologic aquifer.

The third possible aquifer is located in the Oosterhout formation. The aquifer starts at around 320 meters and has thickness between 10 – 35 meters. The Aquifer predominately consists of sand with a big cap layer of predominantly clay above with a thickness between 30 – 50 meters. The thickness of this aquifer varies by quite a lot, being thinner near Oegstgeest, reaching its thickest point near Leiden, and becoming a bit less thick near Zoeterwoude.

4.3.2 Closer look at the formations using the appelboor tool

DINOloket provides a tool called “appelboor”. This tool makes it possible to make a profile at a certain position of the subsurface using one of the previously mentioned modeling tools. It also gives an indication of the horizontal conductivity and the vertical conductivity of the varying layers. Figure 5 gives a profile in between Leiden and Leiderdorp modeled using REGIS II v2.2 and the “appelboor” tool.

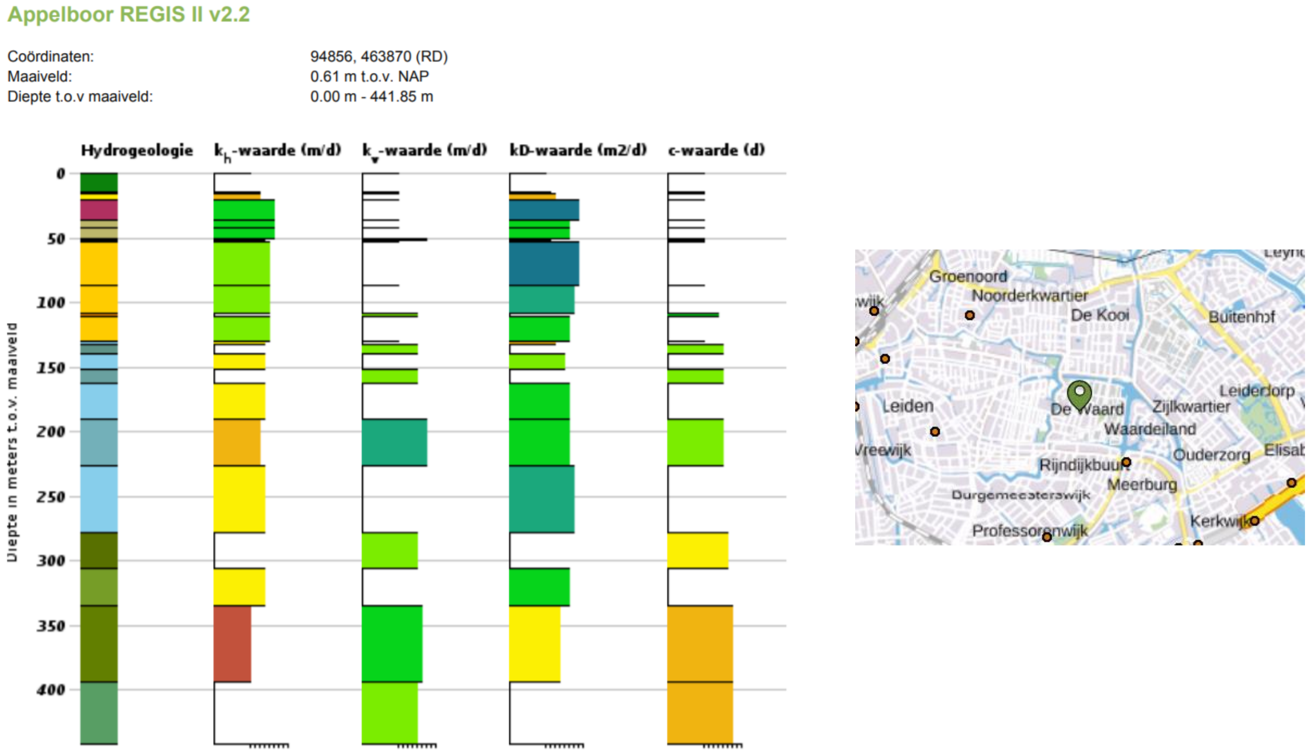

Appelboor REGIS II v2.2

Coördinaten:	94856, 463870 (RD)
Maaiveld:	0.61 m t.o.v. NAP
Diepte t.o.v maaiveld:	0.00 m - 441.85 m

Figure 5: Appelboor profile modeled using REGIS II v2.2 in between Leiden and Leiderdorp

The legend for this profile can be found in appendix B.4. The profile indicates that all three aquifers have a high enough horizontal conductivity and a low vertical conductivity to fit the part of an ideal geology.

4.4 Conclusion

Both the Maassluis formation and the Oosterhout formation look promising for having a potential aquifer usable for an HT-ATES system. The two aquifers in the Maassluis formation and the aquifer located at the Oosterhout formation fit all the requirements.

The deciding factor is the placement of the HT-ATES in between the crossroads. Depending on the location, the aquifer thickness varies considerably. The thickness of the aquifer should be sufficient enough to bear the injected volume of water needed to store the heat via an HT-ATES system computed in chapter 3.2 with minimal heat losses.

All the potential aquifers and their parameters are listed in table 6.

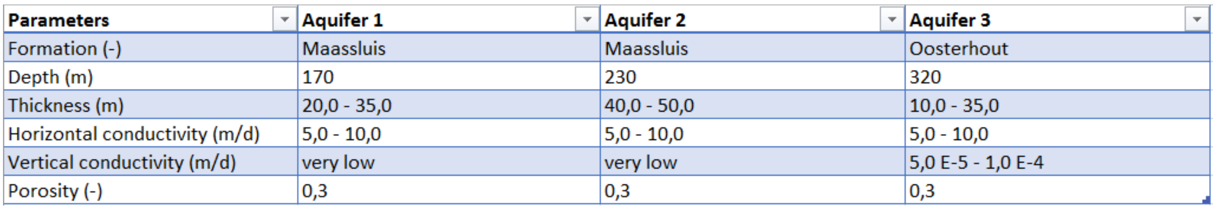

Parameters	Aquifer 1	Aquifer 2	Aquifer 3
Formation (-)	Maassluis	Maassluis	Oosterhout
Depth (m)	170	230	320
Thickness (m)	20,0 - 35,0	40,0 - 50,0	10,0 - 35,0
Horizontal conductivity (m/d)	5,0 - 10,0	5,0 - 10,0	5,0 - 10,0
Vertical conductivity (m/d)	very low	very low	5,0 E-5 - 1,0 E-4
Porosity (-)	0,3	0,3	0,3

Table 6: All the potential aquifers found via interpretation of the subsurface and their parameters

5: Preliminary design of HT-ATES system

In this chapter, a preliminary design of an ATES system is made based on the injected volume of water and pumping rates computed in chapter 3. First, the number of wells per scenario for each potential aquifer identified in chapter 4 is computed. Then, the screen length over thermal radius ratio and area-to-volume ratio is computed per scenario to determine the efficiency. Finally, the data computed will determine the most suitable aquifer to use for this potential HT-ATES.

5.1 Number of wells

Now that the pumping rate and the volume of water is known per different scenario, an estimation of the number of wells per scenario can be computed for each potential aquifer found in chapter 4. To do this, first the design pumping velocity for one well needs to be known. The design pumping velocity per scenario for one well can be computed using equation (5.1) :

$$v_d = 1000 * (\frac{k}{150})^{0.6} * \sqrt{\frac{v_v}{2 * MFI_{mea} * u_{eq}}} \qquad (5.1)$$

With v_d being the design velocity in meters per hour (m/h), k being the horizontal conductivity in meters per day (m/d), v_v being the blockage speed in meters per year (m/a), MFI_{mea} the Modified Fouling Index (-) and u_{eq} the amount of full load hours (h).

All these values are known using the dutch guidelines for ATES well design [18]. Clogging speed is estimated to be 0.1 m/a. MFI_{mea} is estimated to be 2 and the full load hours are assumed to be the number of hours that the ATES system is pumping at full capacity (Scenario 1: 3600 hours; Scenario 2 and 3: 4320 hours). The horizontal conductivity of the different aquifers, according to chapter 3.3, has a minimum value of 5 m/d and a maximum value of 10 m/d. Thus, a minimum design velocity and a maximum design velocity is computed.

Next, the pumping rate required for one well needs to be computed. This is done with equation (5.2):

$$Q_d = v_d * A \qquad (5.2)$$

With Q_d the pumping rate for one well in cubic meters per hour (m^3/h) and A the area of the well in squared meters (m^2). The area of the well, A, can be computed using equation (5.3):

$$A = 2 * \pi * r_{well} * h \qquad (5.3)$$

With r_{well} the radius of the well in meters (m) and h being the thickness of the aquifer in meters (m). In Holland, the standard for the radius of a well can be up to 1 meter. Due to the high total pumping rate required, the radius of the well is assumed to be 1 m. The thickness of the aquifer, according to chapter 4.3, varies per potential aquifer. Thus, for each potential aquifer an area is computed

From the pumping rate for one well, an estimate of the number of wells required to achieve the desired total pumping velocity per aquifer is made using equation (5.4):

$$N = \frac{Q_{tot}}{Q_d} * 2 \qquad (5.4)$$

With N representing the number of wells and Q_{tot}, the total pumping rate required per scenario found in chapter 3.2 (m^3/h). To take into account the extra number of cold wells needed, the ratio is multiplied by a factor of 2.

Per scenario and for each potential aquifer, the minimum and maximum number of wells can now be computed. An overview of the number of wells required per scenario and potential aquifer are given in tables 7 till 9.

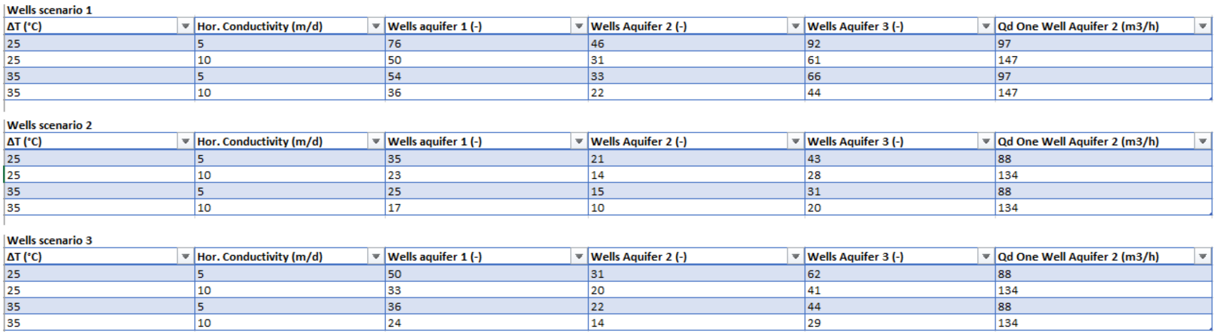

Wells scenario 1

ΔT (°C)	Hor. Conductivity (m/d)	Wells aquifer 1 (-)	Wells Aquifer 2 (-)	Wells Aquifer 3 (-)	Qd One Well Aquifer 2 (m3/h)
25	5	76	46	92	97
25	10	50	31	61	147
35	5	54	33	66	97
35	10	36	22	44	147

Wells scenario 2

ΔT (°C)	Hor. Conductivity (m/d)	Wells aquifer 1 (-)	Wells Aquifer 2 (-)	Wells Aquifer 3 (-)	Qd One Well Aquifer 2 (m3/h)
25	5	35	21	43	88
25	10	23	14	28	134
35	5	25	15	31	88
35	10	17	10	20	134

Wells scenario 3

ΔT (°C)	Hor. Conductivity (m/d)	Wells aquifer 1 (-)	Wells Aquifer 2 (-)	Wells Aquifer 3 (-)	Qd One Well Aquifer 2 (m3/h)
25	5	50	31	62	88
25	10	33	20	41	134
35	5	36	22	44	88
35	10	24	14	29	134

Tables 7 till 9: Number of wells required per scenario for each potential aquifer and required pumping rate for one well used in aquifer 2

From tables 7 till 9 it can be concluded that aquifer 2 requires the least number of wells per scenario. This is due to its higher thickness compared to aquifer 1 and 3. This makes it the most suitable aquifer for this HT-ATES system. Thus, for further calculations in this chapter, results are only computed per scenario for aquifer 2.

5.2 Thermal Radius, surface area and footprint

With the volumes of water known, the thermal radius of the wells can be calculated per scenario for aquifer 2. To compute the thermal radius, equation (5.5) is used [19]:

$$R_{th} = \sqrt{\frac{c_w * V_{in}}{c_{aq} * \pi * l}} = 0{,}66 * \sqrt{\frac{V_{in}}{n * \pi * l}} \qquad (5.5)$$

With R_{th} the thermal radius in meters (m), V_{in} being the infiltrated volume of water in cubic meters (m^3), n is the porosity of the aquifer (-), c_w and c_{aq} the specific heat capacity of water and the saturated porous media respectively (J/kg*K) and l the filter length screen (m).

For the porosity of the aquifer, n, a value is assumed of 0,3 [20] and due to the high volume of water injected the filter length screen is assumed to be the thickness of the different potential aquifers, which can be found in chapter 4.4.

From the thermal radius, the total thermal footprint (A_{foot}) of the wells can now be computed using equation (5.6):

$$A_{foot} = \pi * R_{th}^2 \qquad (5.6)$$

Another area of interest is the total surface area of the thermal cylinder (A_{cyl}) and the volume of the stored heat volume (V), which can be computed using equations (5.7) and (5.8) [19]:

$$A_{cyl} = (2 * \pi * R_{th}^2) + (2 * \pi * R_{th} * l) \qquad (5.7)$$

$$V = \pi * R_{th}^2 * l \qquad (5.8)$$

The thermal radii, footprints, surface areas and volumes per scenario for aquifer 2 are given in tables 10 through 12.

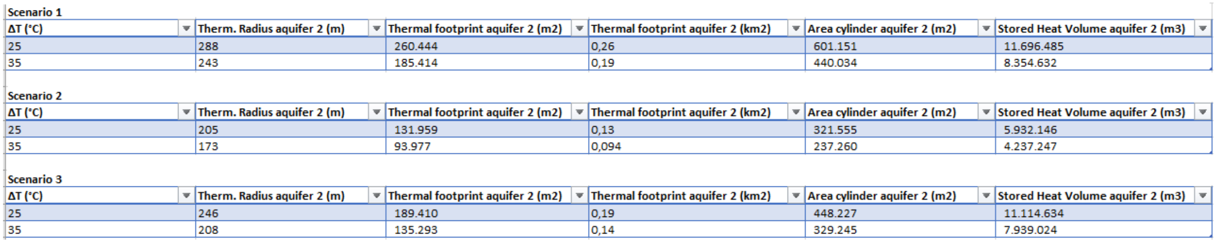

Scenario 1

ΔT (°C)	Therm. Radius aquifer 2 (m)	Thermal footprint aquifer 2 (m2)	Thermal footprint aquifer 2 (km2)	Area cylinder aquifer 2 (m2)	Stored Heat Volume aquifer 2 (m3)
25	288	260.444	0,26	601.151	11.696.485
35	243	185.414	0,19	440.034	8.354.632

Scenario 2

ΔT (°C)	Therm. Radius aquifer 2 (m)	Thermal footprint aquifer 2 (m2)	Thermal footprint aquifer 2 (km2)	Area cylinder aquifer 2 (m2)	Stored Heat Volume aquifer 2 (m3)
25	205	131.959	0,13	321.555	5.932.146
35	173	93.977	0,094	237.260	4.237.247

Scenario 3

ΔT (°C)	Therm. Radius aquifer 2 (m)	Thermal footprint aquifer 2 (m2)	Thermal footprint aquifer 2 (km2)	Area cylinder aquifer 2 (m2)	Stored Heat Volume aquifer 2 (m3)
25	246	189.410	0,19	448.227	11.114.634
35	208	135.293	0,14	329.245	7.939.024

Tables 10 till 12: The thermal radii, footprints, surface areas and volumes per scenario for aquifer 2

5.3 L/R and A/V

With the thermal radius calculated, the dimensionless ratio of the filter screen length and the thermal radius (L/R_{th}) can be computed. This ratio is an indicator for the thermal recovery efficiency of an ATES system for a stored thermal volume. The optimal value of L/R_{th} is between 1 and 4 [19].

Another ratio of interest is the surface area – volume ratio (A_{cyl}/V). To gain the highest efficiency, the water volume should be in a shape that has the smallest area. Spheres have the smallest surface area that encloses a given volume. Thus, for a high efficiency, the shape of the water volume should be close to the shape of a sphere. The lower the number, the higher the efficiency.

The L/R_{th} and A_{cyl}/V ratios per scenario for aquifer 2 are computed in tables 13 till 15.

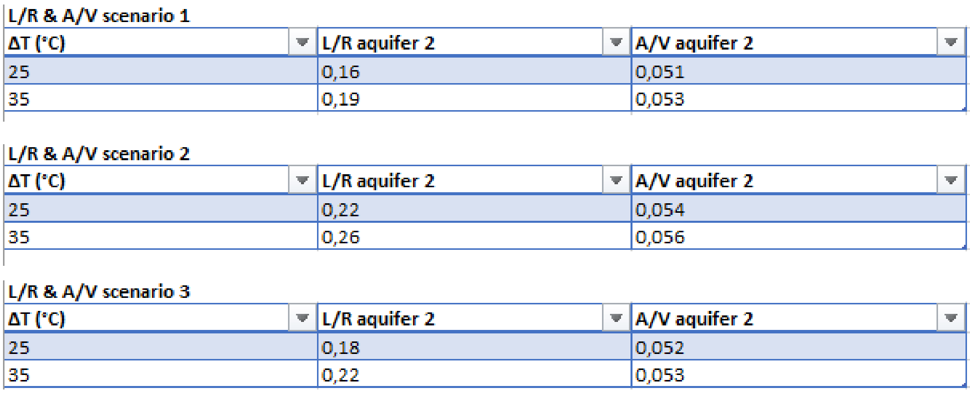

L/R & A/V scenario 1

ΔT (°C)	L/R aquifer 2	A/V aquifer 2
25	0,16	0,051
35	0,19	0,053

L/R & A/V scenario 2

ΔT (°C)	L/R aquifer 2	A/V aquifer 2
25	0,22	0,054
35	0,26	0,056

L/R & A/V scenario 3

ΔT (°C)	L/R aquifer 2	A/V aquifer 2
25	0,18	0,052
35	0,22	0,053

Tables 13 till 15: The L/R_{th} and A_{cyl}/V ratios per scenario for aquifer 2

5.4 Conclusion

With all the parameters computed, it can be concluded that aquifer 2 located in the Maassluis formation will be the best suited as a potential aquifer for an HT-ATES system. This is due to its high thickness, which lies between 45-50 meters. Due to the high thickness, the aquifer needs the least number of wells per scenario. Aquifer 1 and aquifer 3 are less thick. More wells are needed per scenario, leading to an increase in costs. Concluding that aquifer 2 is the most suitable for an HT-ATES system near Leiden.

One of the things to note is that the L/R_{th} ratios are quite low compared to the optimal relation between 1 and 4 for aquifer 2 [19]. However, due to the large storage volumes, the A_{cyl}/V ratios for aquifer 2 are low and indicate high efficiency

6: Design challenges

This chapter will describe the different design challenges that have to be faced when installing an HT-ATES system. In this chapter, the mechanism in density difference between hot water and cold water will be explained, and how it can result in heat loss. Clogging of the aquifer can also occur. This chapter will explain the mechanism and how to prevent it. Finally, it is described how to increase the efficiency of the HT-ATES system.

6.1 Density differences

In general, there are three stages during the buffering via an HT-ATES system:

1. Hot water gets pumped into the suitable aquifer
2. Hot water stays in the aquifer
3. How water gets extracted from the suitable aquifer

Each stage is influenced by the effect of a density driven flow.

6.1.1 Stage one

During this stage, groundwater might already be present in the aquifer. This groundwater has a colder temperature than the injected hot water. In general, when temperature increases, density decreases. Thus, there is a difference in density occurring between the colder, already present, groundwater and the injected hot water. This can cause a, so called, thermal front to occur in the aquifer. The thermal front is illustrated in figure 6. The thermal front is a boundary separating the two masses of water with different densities. This thermal front will cause heat loss to occur. The bigger the temperature difference, the bigger the density difference. This causes a steeper front angle to occur. When the angle gets steeper, more heat loss occurs [21].

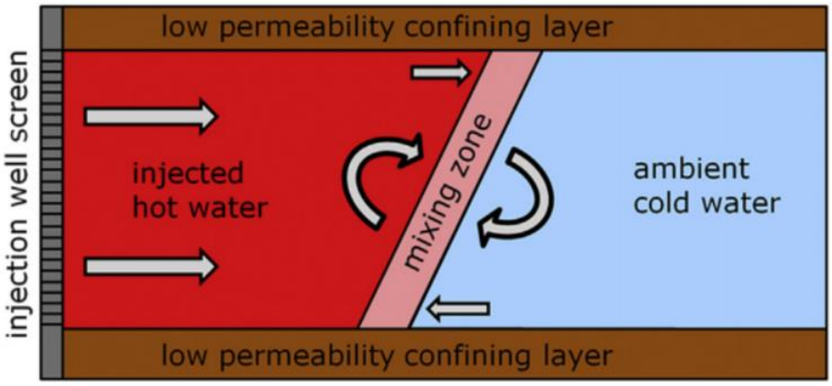

Figure 6: Thermal front occurring in an aquifer due to the difference in densities between the injected hot water and cold groundwater present. (Schout et al [20])

6.1.2 Stage two

During this stage, the hot water stays in the aquifer as a buffer for the higher peak demands during wintertime. During this phase, the thermal front caused by the colder groundwater and the injected hot water still occurs, as well as tilting of the angle of the thermal front. Equation (6.1) [21] describes this tilting effect:

$$t_0 = \frac{H}{\sqrt{k_a^h * k_a^v}} * \frac{C_a}{C_w} * \frac{\pi^2(\mu_0 + \mu_1)}{32G(\rho_0 - \rho_1)g} \qquad (6.1)$$

Where t_0 is the time in seconds for tilting of an initially vertical front to reach 60° (s), H is the aquifer thickness in meters (m), k_a^h and k_a^v are the horizontal and vertical permeability (m^2), C_a and C_w the volumetric heat capacities of the aquifer and water ($J/(m^3*°C)$), μ_0 and μ_1 are the dynamic viscosities of the groundwater present and the injected water ($kg/(m*s)$), ρ_0 and ρ_1 indicating the densities of the groundwater present and the injected water (kg/m^3), G is the Catalan's constant (0,916) and g is the gravitational constant of earth ($9{,}81\ m/s^2$).

One of the things that can be noted by this equation, that next to the density difference, dynamic viscosity difference between the groundwater present and the injected water also has an effect of the tilting time. From (6.1) it can be seen that if the dynamic viscosity difference increases, the tilting time increases. In general, dynamic viscosity decreases due to higher temperatures [26]. Thus, for an HT-ATES system, higher temperatures can also cause a decrease in dynamic viscosity difference and a decrease in tilting time.

6.1.3 Stage three

During this stage, hot water gets extracted from the aquifer to fulfill the peak demands during wintertime. As discussed before, due to the density driven flow, a tilting thermal front occurs. This causes hot water in top part of the aquifer to not reach the well, while cold water at the bottom of the aquifer succeeds in reaching the well [21]. This effect can be seen in figure 6. This effect caused by the density driven flow will cause heat loss to occur.

6.1.4 Storage efficiency

Due to the effect of the density driven flow, there will always be heat losses. Therefore, during calculations in heat storage, one needs to take into account the storage efficiency. The storage efficiency is the ratio between the total heat storage and what amount of that stored heat can get lost due to the effect of heat loss. According to [12], the storage efficiency for an HT-ATES system lies between 50 – 70%.

6.2 Clogging

Another problem that can occur is clogging of the aquifer. This happens due to precipitation of carbonates due to high temperature heat storage. This is a problem that one might recognize from daily practice. For instance: scaling of the showerhead due to hot showers or scaling occurring in the kettle due to the heating from cold water to boiling water.

The solubility of lime ($CaCo_3$) in water decreases with increasing temperatures [23]. As stated before, during high temperature storage, water is stored with temperatures above 60°C. Due to the high temperature of the water, lime minerals contained in the hot water cannot be dissolved. This can cause scaling to happen in the aquifer, causing insufficient flow of the water to occur.

There are ways to combat this low solubility effect. One of the ways is the dosage of a hydrochloric acid. This causes the pH of the water to decrease, making the water more able to dissolve the lime minerals. This way of combating the problem is already in practice in the Netherlands with good results. Possible drawbacks of this methods are the negative effect on the pH and the increase in chlorine concentration of the water.

Another way to combat clogging is the use of ion exchange. A vessel filled with negatively charged resin granules are equilibrated using a NaCl solution. Due to the negative charge, Na^+ ions will stick to negatively charged granules. When the hot water passes along the granules, a cation exchange occurs, swapping the Na^+ ions with other cations, such as Ca^{2+}. This withdraws the Ca^{2+} ions from the water and replaces it with Na^+ ions. In theory, this can lead to a decrease in scaling. In practice however, the method is very labor intensive and the risk of clogging still occurs

6.3 Efficiency increase

A way to increase the storage efficiency is to decrease the density difference between the hot injected water and the colder groundwater. A proposed way to do this is to inject hot water with a high concentration of dissolved salts in the aquifer [24]. The added salt concentration will cause the density of the hot water to increase again, causing a reduction in the density difference between the hot and cold water which increases the storage efficiency. Thus, a higher salt concentration in the hot injected water can lead to an increase of the storage efficiency.

Another way to increase the storage efficiency is to increase the pumping rate. During stage 1 of an HT-ATES system, there are two types of convections occurring. The “forced convection” (pumping of hot water) and the “free convection” (density effects). According to [22], one of the ways to prevent the angle of the thermal front to increase is to increase the pumping rate. The “forced convection” will then start to act more like a vertical line due to the “forced” convection exceeding the ”free” convection. Thus, a way to prevent to prevent this steep angle in the first step is to have the highest pumping rate possible.

Lastly, multiple storage cycles will also increase the efficiency. A storage cycle consists of injecting the hot water into the aquifer and extracting it from the aquifer. This increase in efficiency is due to losses from the previous cycle reducing the losses of the current cycle [22]

7: Discussion and further recommendations

With this being the first step concerning HT-ATES suitability in Holland-Rijnland, there are some points of improvement and gaps for a further research concerning the topic. The most important improvements and gaps are listed in this chapter.

7.1 Layout Heat Network & Urban Areas

The current projected heat network of Holland-RIjnland [8] is a proposed heat network, indicating that the layout of the heat network throughout the area can change in the future. Layout changes can cause a change in the potential geographical area for placement of an HT-ATES system. A different geographical area has a different geology beneath the surface, which then needs a new detailed interpretation. Further changes in the proposed heat network need to be incorporated within future studies.

One of the deciding factors is the placement of the HT-ATES system within the crossroads. The thickness of the potential aquifer varies, depending on the placement. Placement however, is also dependent on how highly urban the location is, with a highly urban area not recommended for placement of an HT-ATES system. In the case of this research, a simplification is made by not taking the urbanization of the location into account. Further research is recommended on locating the best possible, single placement of an HT-ATES system in the area indicated in appendix B.3 by taking urbanization into account.

7.2 Heat demand

Heat demands per month per scenario are assumed based on data from KNMI [9] in combination with the potential scenario's gained from Holland-Rijnland [8]. Thus, the heat demand per scenario can vary in the future. This all amounts to uncertainties in calculations using the heat demand throughout the year. For future works, more detailed heat demands throughout the year should be in place. Changes in heat demand also need implementation as it will impact potential heat storage.

7.3 Parameters

Due to lack of data, certain parameters such as full load hours and peak power that are used now for computing certain data, either had to be assumed or estimated. This leads to uncertainties in data such as the number of wells and the thermal recovery efficiency. For future works, these uncertainties have to be reduced.

7.4 Economics

This report does not involve an economic prospect for an HT-ATES system near Leiden. This was chosen not to do due to lack of detailed information on this topic. Due to the lack of an economic prospect, many assumptions have to be made during future calculations of the economic prospect of an HT-ATES project near Leiden. Nevertheless, the economic prospect of an HT-ATES system near Leiden remains one of the most important criteria in deciding the viability of such a project. For an economic prospect of the project, a detailed plan needs to be set up with more information about certain equipment used, the amount of hot and cold water storage and the amount of full load hours.

8: Conclusion

The goal of this research is to see if the deep underground near Leiden is suitable in order to store the heat supplied from the port of Rotterdam. From this research, it can be concluded that three aquifers are suitable for the use of an HT-ATES system, with the aquifer located at 230 meters depth in the Maassluis formation being the most suitable. Per scenario, this aquifer needs the least number of wells for the desired pumping rate. Depending on the scenario, the aquifer has a thermal recovery efficiency ratio between 0,16 – 0,26 and an area – to – volume ratio between 0,051 – 0,056.

Appendix

Appendix A: Figures heat demand per scenario

A.1: Heat demand and heat supply over a year for scenario 1

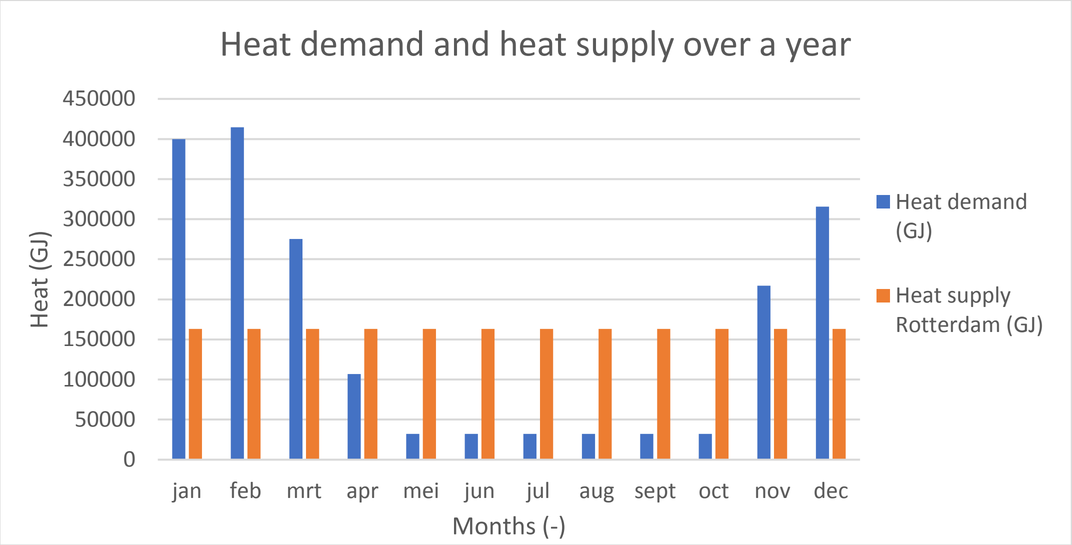

A.2: Heat demand and heat supply over a year for scenario 2

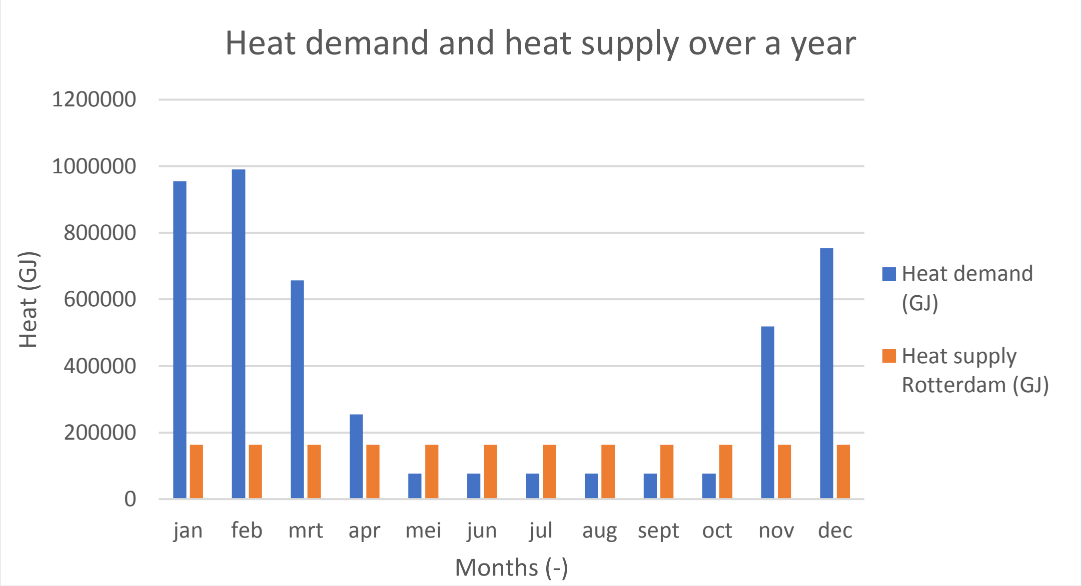

A.3: Heat demand and heat supply over a year for scenario 3

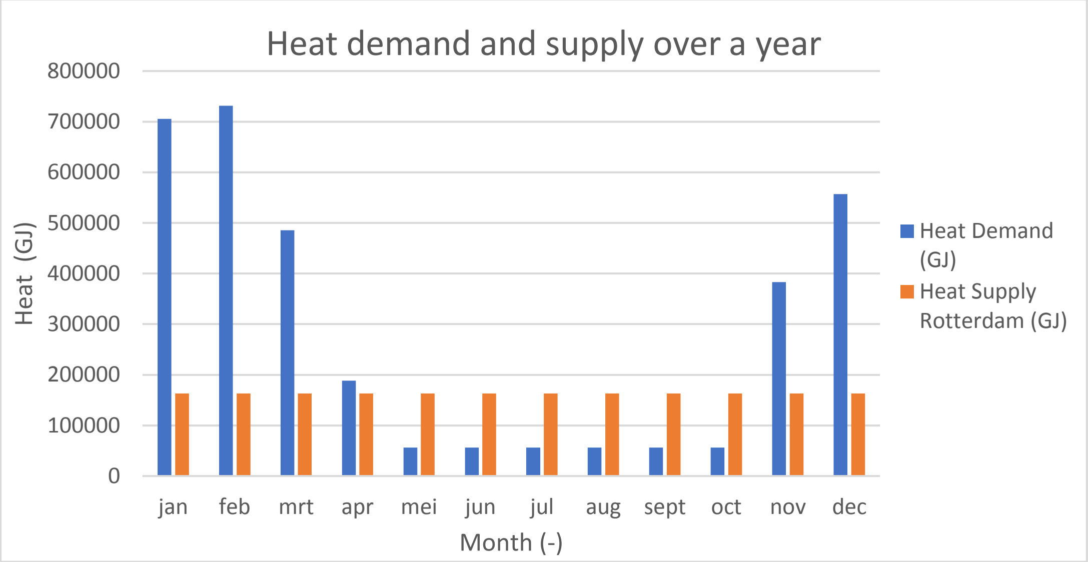

Appendix B: Proposed area & legends

B.1: Area considered for the high temperature heating network

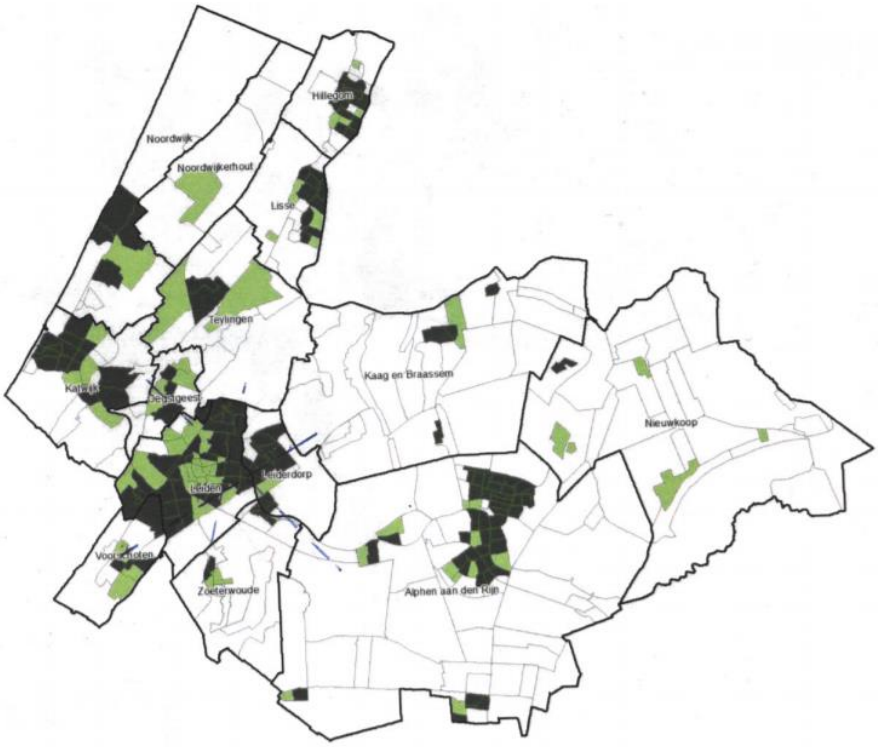

B.2: Proposed heat network throughout the area considered

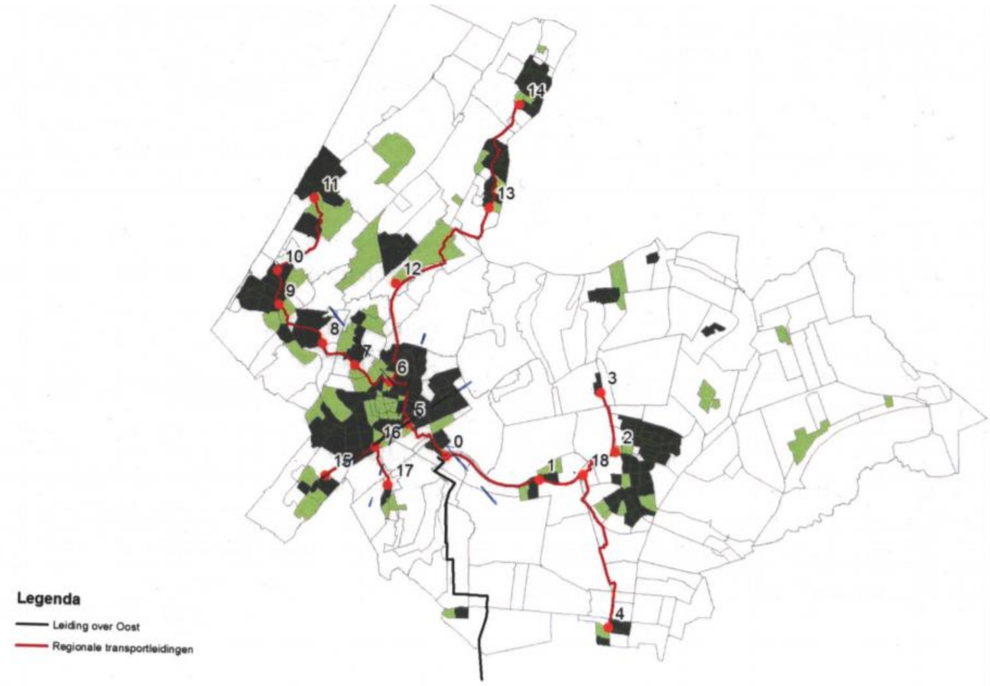

B.3: Cross section lines through the crossroads between Leiden, Leidendorp and Zoeterwoude

B.4 Legends for figure 4 and Appelboor profile

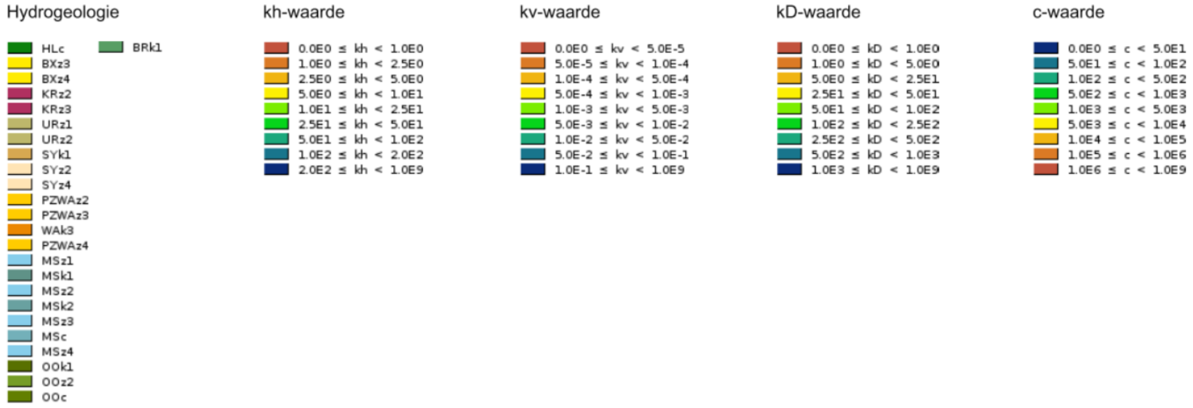

Hydrogeologie

- 🟩 HLc
- 🟨 BXz3
- 🟨 BXz4
- 🟪 KRz2
- 🟪 KRz3
- 🟫 URz1
- 🟫 URz2
- 🟫 SYk1
- ⬜ SYz2
- ⬜ SYz4
- 🟨 PZWAz2
- 🟨 PZWAz3
- 🟧 WAk3
- 🟨 PZWAz4
- 🟦 MSz1
- 🟩 MSk1
- 🟦 MSz2
- 🟦 MSk2
- 🟦 MSz3
- 🟦 MSc
- 🟦 MSz4
- 🟩 OOk1
- 🟩 OOz2
- 🟩 OOc
- 🟩 BRk1

kh-waarde	kv-waarde	kD-waarde	c-waarde
🟥 0.0E0 ≤ kh < 1.0E0	🟥 0.0E0 ≤ kv < 5.0E-5	🟥 0.0E0 ≤ kD < 1.0E0	🟦 0.0E0 ≤ c < 5.0E1
🟧 1.0E0 ≤ kh < 2.5E0	🟧 5.0E-5 ≤ kv < 1.0E-4	🟧 1.0E0 ≤ kD < 5.0E0	🟦 5.0E1 ≤ c < 1.0E2
🟧 2.5E0 ≤ kh < 5.0E0	🟧 1.0E-4 ≤ kv < 5.0E-4	🟧 5.0E0 ≤ kD < 2.5E1	🟩 1.0E2 ≤ c < 5.0E2
🟨 5.0E0 ≤ kh < 1.0E1	🟨 5.0E-4 ≤ kv < 1.0E-3	🟨 2.5E1 ≤ kD < 5.0E1	🟩 5.0E2 ≤ c < 1.0E3
🟩 1.0E1 ≤ kh < 2.5E1	🟩 1.0E-3 ≤ kv < 5.0E-3	🟩 5.0E1 ≤ kD < 1.0E2	🟩 1.0E3 ≤ c < 5.0E3
🟩 2.5E1 ≤ kh < 5.0E1	🟩 5.0E-3 ≤ kv < 1.0E-2	🟩 1.0E2 ≤ kD < 2.5E2	🟨 5.0E3 ≤ c < 1.0E4
🟩 5.0E1 ≤ kh < 1.0E2	🟩 1.0E-2 ≤ kv < 5.0E-2	🟩 2.5E2 ≤ kD < 5.0E2	🟧 1.0E4 ≤ c < 1.0E5
🟦 1.0E2 ≤ kh < 2.0E2	🟦 5.0E-2 ≤ kv < 1.0E-1	🟦 5.0E2 ≤ kD < 1.0E3	🟧 1.0E5 ≤ c < 1.0E6
🟦 2.0E2 ≤ kh < 1.0E9	🟦 1.0E-1 ≤ kv < 1.0E9	🟦 1.0E3 ≤ kD < 1.0E9	🟥 1.0E6 ≤ c < 1.0E9

References

[1] Zillman J. & Sherwood S. The enhanced greenhouse effect, 07-11-2017. URL: https://www.science.org.au/curious/earth-environment/enhanced-greenhouse-effect

[2] Hannah Ritchie and Max Roser. Renewable Energy, 2019 URL: https://ourworldindata.org/renewable-energy

[3] European Environment Agency. European Environment Agency: Primary consumption by fuel, 21-12-2018. URL: *https://www.eea.europa.eu/data-and-maps/indicators/primary-energy-consumption-by-fuel-6/assessment-2*

[4] Export.gov. Export.gov : Netherlands – Energy, 24-10-2018. URL: https://www.export.gov/article?id=Netherlands-Energy

[5] EBN. EBN: De energiebalans in Nederland, 2019. URL: https://www.ebn.nl/energietransitie/energiebalans-van-nederland/

[6] Government of the Netherlands. Government of the Netherlands: Central government encourages sustainable energy, 2019. URL: https://www.government.nl/topics/renewable-energy/central-government-encourages-sustainable-energy

[7] Gemeente Leiden. Gemeente Leiden: De Leidse Warmtevise Inspraakversie, 13-06-17. URL: https://www.gagoed.nl/uploads/20170606-Warmtevisie-Leiden-VERSIE-VOOR-INSPRAAK-DEFINITIEF.pdf

[8] Rob Bremer. Holland-Rijnland: Warmtevisie HT-Restwarmte, 04-03-2019.

[9] KNMI. KNMI: Maand- en jaarwaarden,2019. URL: https://www.knmi.nl/nederland-nu/klimatologie/maandgegevens

[10] Engineering ToolBox, Water - Thermophysical Properties (2003). URL: https://www.engineeringtoolbox.com/water-thermal-properties-d_162.html

[11] Hacking, T., (2017). The Suitability of a High Temperature Aquifer Thermal Energy Storage on the TU-Delft Campus. URL: http://resolver.tudelft.nl/uuid:0d4f71b9-dc46-4fa3-a7f7-28c4888a38bf

[12]SKB. SKB: Position Paper Hogetemperatuuropslag, 05-2013. URL: https://soilpedia.nl/Bikiwiki%20documenten/SKB%20Projecten/2068%20Hogetemperatuuropslag%20in%20de%20bodem/7751%20SKB%20HTO.pdf

[13] Overheid.nl. Mijnbouwwet: Hoofdstuk 2, 05-01-16. URL: https://wetten.overheid.nl/BWBR0014168/2016-05-01#Hoofdstuk2

[14] Pluymakers M. et al. TNO – Hoge temperatuur opslag in ondiepe ondergrond, 01-11-13. URL: https://www.tno.nl/media/2491/tno_rapport-hoge-temperatuur-opslag-in-ondiepe-ondergrond.pdf

[15] DINO-Loket. Dino-loket, 06-2019. URL https://www.dinoloket.nl

[16] DINO-Loket. Dino-loket, 06-2019. URL https://www.dinoloket.nl/formatie-van-maassluis

[17] DINO-Loket. Dino-loket, 06-2019. URL https://www.dinoloket.nl/formatie-van-oosterhout

[18] NVOE Richtlijnen Ondergrondse Energieopslag, november 2006

[19] Bloemendal M. & Hartog N. Analysis of the impact of storage conditions on the thermal recovery efficiency of low-temperature ATES systems, January 2018. URL: https://www.sciencedirect.com/science/article/pii/S0375650517302067

[20] Schout G. et al. The influence of the injection temperature on the recovery efficiency of high temperature aquifer thermal energy storage, 2016. URL: https://dspace.library.uu.nl/handle/1874/331159

[21] Drijver et al. High-temperature aquifer thermal energy storage (HT-ATES) - sustainable and multi-usable, may 2012. URL: https://www.researchgate.net/publication/280727135_High-temperature_aquifer_thermal_energy_storage_HT-ATES_-_sustainable_and_multi-usable

[22] Ward D. J. et al. A theoretical analysis of mixed convection in aquifer storage and recovery: How important are density effects, 20-09-07. URL: https://www.sciencedirect.com/science/article/pii/S0022169407003472

[23] National Lime Association. Fact sheet: Lime Terminology, Standards & Properties, 2017. URL: https://www.lime.org/documents/lime_basics/lime-physical-chemical.pdf

[24] Lopik et al.The use of salinity contrast for density difference compensation to improve the thermal recovery efficiency in high-temperature aquifer thermal energy storage systems, 2016. URL: https://dspace.library.uu.nl/handle/1874/335189

[25] Geotechdata.info. Soil void ratio, 16-11-13. URL: https://www.geotechdata.info/parameter/soil-porosity.html

[26] Engineering ToolBox. Water - Dynamic and Kinematic Viscosity (2004). URL: https://www.engineeringtoolbox.com/water-dynamic-kinematic-viscosity-d_596.html